

Investigation of Flow Separation Control with Dielectric Barrier Discharge Plasma Actuator

J.G. Zheng*, Y.D. Cui*, B.C. Khoo*

* Temasek Laboratories, National University of Singapore, Singapore 117411

Abstract

The flow separation control over a NACA0015 airfoil at high angle of attack with nanosecond dielectric barrier discharge plasma actuator is investigated through numerical simulation. A self-similar plasma model for describing nanosecond pulsed discharge is incorporated into the Reynolds averaged Navier-Stokes equations governing the external airflow. The simulation results show that each discharge induces a spanwise vortex and these vortices resulting from repetitive discharges entrain external flow with high momentum into the separation region over the upper surface and finally leads to the reattachment of separated boundary layer. As a result, the airfoil performance can be improved significantly.

1. Introduction

Flow separation control based on nanosecond (ns) dielectric barrier discharge (DBD) actuator has proved to be an effective actuation technique in many aerodynamic systems. As the typical pulse duration is on the order of tens of nanoseconds, part of electrical energy in each pulse discharge is converted into gas heating within the discharge volume in a short time period of less than $1 \mu\text{s}$ [1]. This leads to the fast heating of near surface gas. As a result, the temperature and pressure in the actuator region increase appreciably, which causes the generation of a micro shock wave. Compared with traditional alternating current (AC) plasma actuator, the nanosecond DBD actuator operates with a fundamentally different mechanism and actually functions via the Joule heating effect [1-3]. It is found from the detailed simulation that for the airfoil leading edge separation control, the discharge produced residual heat triggers the inherent flow instability, causes the generation of spanwise vortices and finally makes the separated flow being reattached. The shock wave introduces transient perturbations to external flow and contributes little to control authority [3]. In the current study, the flow separation control over a NACA 0015 airfoil with a nanosecond DBD actuator is simulated. The airfoil at high angle of attack is deeply stalled. The pulsed discharge is described by a well validated and verified self-similar plasma model, which is loosely coupled with two-dimensional compressible Reynolds averaged Navier-Stokes (RANS) equations solver with Reynolds stress turbulence model to resolve the detailed flow control process. The reattachment of separated flow on airfoil upper surface under the impact of repetitive discharges is simulated and illustrated. It is found that the nanosecond DBD actuator can effectively control the massively separated shear layer over a deeply stalled airfoil, but its efficacy may gradually degrade with further increasing attack angle.

The paper is organized as follows. In Section 2, physical models for plasma discharge and mean flow are presented. The numerical results and discussion are given in Section 3, while conclusion is provided in Section 4.

2. Modelling and Numerics

2.1 Self-similar plasma model

The surface nanosecond plasma discharge is described by a self-similar plasma model, which is derived from 2D drift-diffusion equations with some insignificant physical procedures such as ion motion, electron diffusion, recombination on nanosecond time scale neglected [4]. The resulting model is composed of equations describing parallel and perpendicular components of near wall electric field, E_x and E_y , electron and ion densities, n_{ew} and n_{iw} , and plasma layer thickness parameter $\lambda = 1/\delta$ such that $n_e(x, y) = n_{ew}(x) \exp(-\lambda y) = n_{ew}(x) \exp(-y/\delta)$:

$$\begin{aligned}
\frac{dE_x}{d\xi} &= -\frac{3}{2} \frac{E_x^2}{\varphi} - \frac{e}{\varepsilon_0} (n_i - n_e), & \frac{dE_y}{dy} &= \frac{3}{2} \frac{E_x^2}{\varphi} \\
\frac{dE_y}{d\xi} &= \frac{dE_x}{dy} = \frac{\varepsilon}{h} E_x - \frac{en_e \mu_e E_y}{\varepsilon_0 V} \\
\frac{dn_e}{d\xi} &= \frac{vn_e + \mu_e n_e (dE_x/d\xi) + 3\mu_e n_e (E_x^2/\varphi)/2 - \mu_e \lambda n_e E_y}{V - \mu_e E_x} \\
\frac{dn_i}{d\xi} &= \frac{vn_e}{V} \\
\frac{d\lambda}{d\xi} &= \frac{a}{V} \frac{dv}{dy} \frac{d(\ln v)}{d(\ln E)}
\end{aligned} \tag{1}$$

where, V is the ionization wave speed and $\xi = x + V \cdot t$ is the introduced self-similar variable; φ represents the electric potential at the wall such that $E_x = -d\varphi/d\xi$. For more information on the definition of variables in model system (1) as well as the initial and boundary conditions, the reader is referred to [1, 3-4].

Given the peak pulse voltage U_p and rise time τ_r , which are strongly load-dependent and satisfy the relation $dU/dt \approx E_{x0} V$, the coupled total energy per actuator length in spanwise direction, Q_{couple} , can be predicted by solving the above model system. About 35% of the coupled electrical energy is absorbed by the neutral gas in the discharge region for heating, i.e. $Q_h = \eta \cdot Q_{couple}$ with $\eta = 0.35$. The gas heating energy Q_h is then distributed in the plasma region to obtain the energy density $q_h(x, y)$, which is divided by heating time and then added to the energy equation of external flow as source term to represent the heating effect due to plasma discharge.

2.2 Computational modeling of airflow and numerical method

The mean flow is governed by two-dimensional Reynolds averaged Navier-Stokes (RANS) equations. Reynolds stress turbulence model (RSM) is found to be able to satisfactorily predict both baseline flow and flow control process for a comparison with experiment and therefore is adopted in this study. The power density calculated from heating energy density and heating time [3] is then added to the energy equation as source term to account for the plasma heating effect. The Navier-Stokes equations are discretized using a cell-centered finite volume method on structured mesh. Time-marching is dealt with using a dual-time-stepping strategy for unsteady calculation. A multigrid technique is used to enhance the convergence of a solution.

3. Numerical results and discussion

3.1 Baseline flow

The flow around a NACA0015 airfoil is investigated. The chord length of airfoil is 8cm and freestream speed is 30m/s. The resulting Reynolds number at room temperature of $T=300K$ is 1.5×10^5 . At this Reynolds number, the stall angle of attack (AoA) is around 12° . In this study, we examine a deeply stalled case with $AoA=20^\circ$. A structured mesh of 750×250 (circumferential \times normal) is used in the simulation.

The baseline flow without control is resolved first and vorticity field superimposed with streamlines in Figure 1 shows the transient flow pattern. As shown in Figure 1, the high attack angle leads to a massively separated flow over the upper surface of airfoil. The basic flow structures include a strong trailing edge vortex, some secondary separated vortices over mid-portion of airfoil upper surface and a leading edge shear layer. The vortices of opposite signs alternatively shed from airfoil, forming a Kármán vortex street in wake. It is well known that flow separation beyond stall and stall itself is notoriously difficult to predict. However, the current simulation with Reynolds stress turbulence model produces relatively good results. The irregular flow features of post-stall flow are well captured. RSM is superior to other RANS turbulence models in the calculation of certain airfoil flows.

3.2 Flow control process

The instantaneous flow in Figure 1 is our starting point for flow separation control. The nanosecond DBD actuator is mounted on the leading edge of airfoil and is very close to the separation point of boundary layer. The pulse discharge frequency is $f = 1000\text{Hz}$, which together with airfoil chord length and freestream speed results in a reduced frequency of $f^+ = 2.67$. The peak pulse voltage is 20kV and pulse duration is around 50 nanoseconds.

The sequence of vorticity contours overlaid with streamlines in Figure 2 shows that the massively separated shear layer reattaches on the airfoil upper surface under the impact of a few pulse discharges. Our previous study indicates that the discharge generated shock wave contributes little to the flow control authority and therefore is not examined here. Figure 2(a) illustrates that by time $t=1T_p$ with $T_p = 1/f$, the first pulse has induced a spanwise vortex. This vortex destroys the original shear layer and entrains mean flow with higher speed into the separation region. It is produced by triggering inherent flow instability and the residual heat rather than shock wave plays a dominant role in the vortex generation. It is observed from Figure 2(b) that the second pulse generates a similar vortex and the original separation region further collapses. After the implementation of 6 pulses, the separated flow is partially reattached and characterized by a train of downstream moving vortices and a small separation bubble near the leading edge. Figure 2 depicts the early and intermediate stages of flow control process. Finally, a quasi-periodic flow pattern is established as shown in Figure 3 where the transient flow field after 30 pulse discharge is illustrated. It is seen that a big separation bubble reappears near the trailing edge. This is different from the scenario associated with lower attack angle, where such large separation region near trailing edge has been suppressed. Actually, with increasing the attack angle, the flow control authority degrades and the actuator is not able to suppress the whole separated shear layer, especially at the trailing edge.

The aerodynamic performance of airfoil is also improved. When the control is implemented, the value of lift coefficient is increased from 0.8 to 1.15, while drag coefficient is reduced from about 0.4 to 0.2.

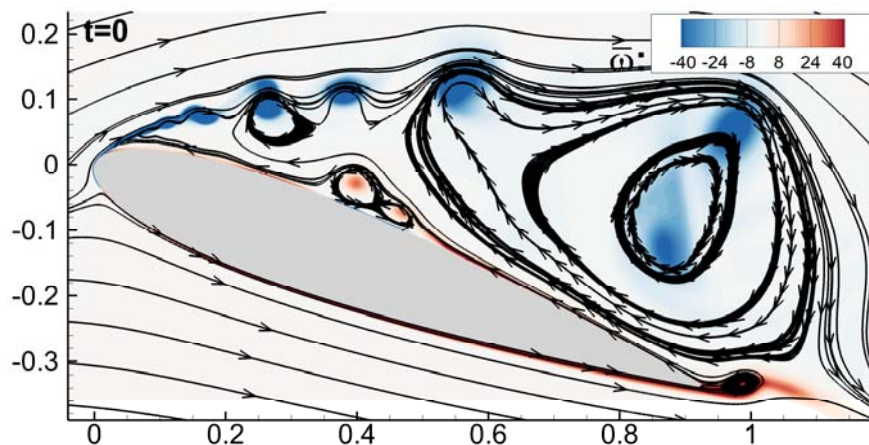


Figure 1: The baseline flow without control, $Re=1.5 \times 10^5$, $AoA=20^\circ$.

4. Conclusion

Numerical simulation is performed to investigate the leading edge separation control over a NACA0015 airfoil based on nanosecond plasma actuator. The efficacy of this type of actuator is demonstrated for the effective and efficient control of deeply stalled flow. The discharge induced spanwise vortices are essential for the effective flow actuation. However, the control authority may degrade with increasing angle of attack.

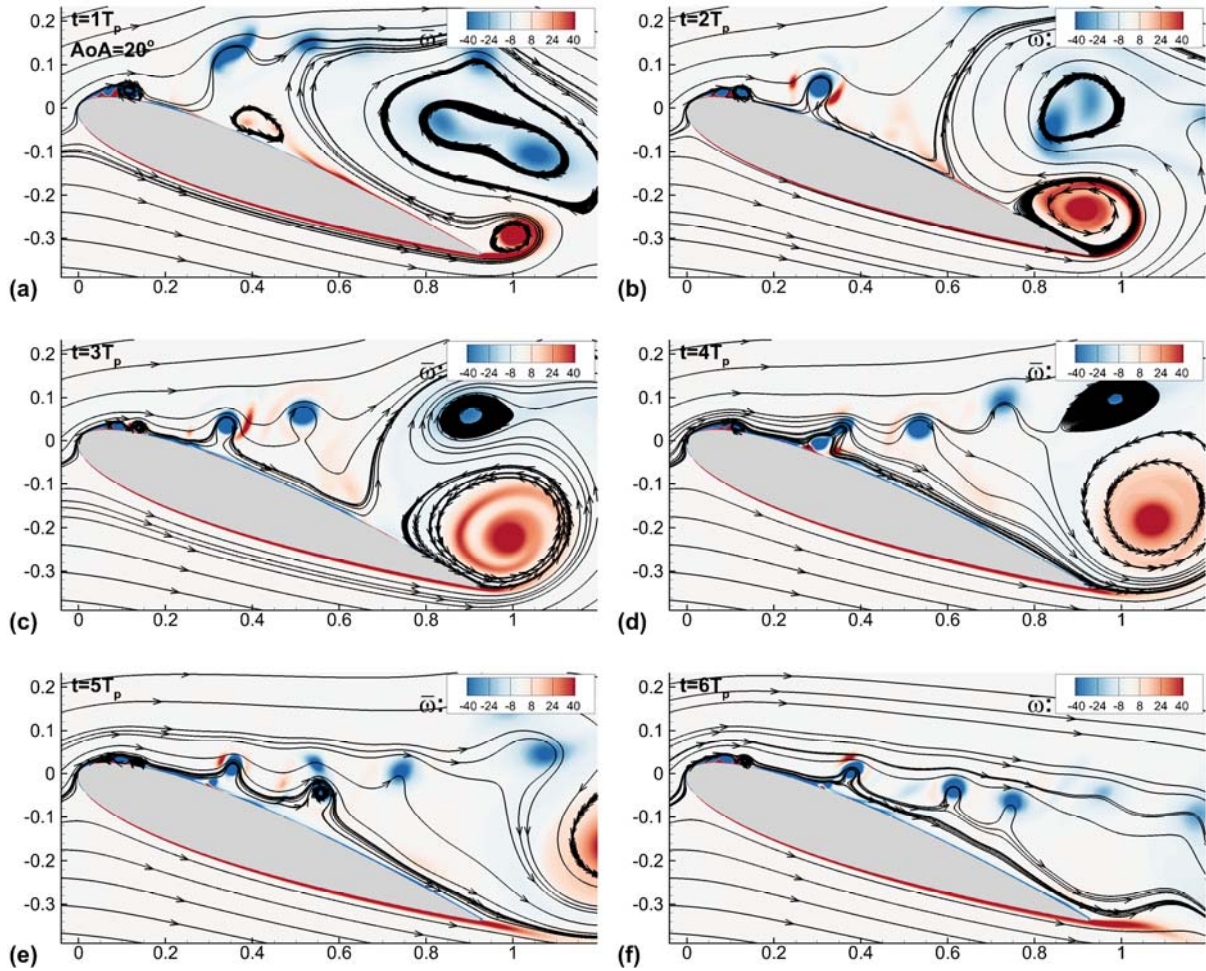


Figure 2: The vorticity field superimposed with streamlines shows the flow reattachment process.

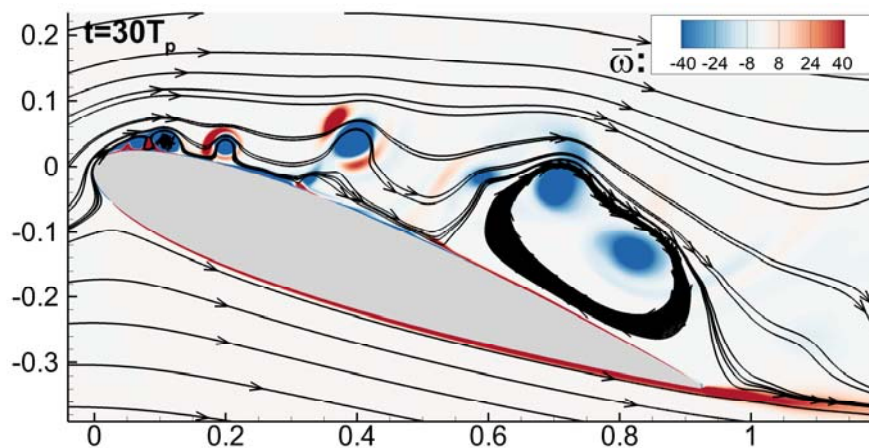


Figure 3: The transient flow field after the implementation of 30 pulses.

References

- [1] Zheng, J.G., Z. J. Zhao, J. Li, Y. D. Cui, and B. C. Khoo. 2014. Numerical simulation of nanosecond pulsed dielectric barrier discharge actuator in a quiescent flow. *Phys. Fluids*. 26(3): 036102.

- [2] Zheng, J.G., J. Li, Y. D. Cui, Z. J. Zhao, and B. C. Khoo. 2016. Numerical study of nanosecond pulsed plasma actuator in laminar flat plate boundary layer. *Commun. Comput. Phys.* 20(5): 1424-1442.
- [3] Zheng, J.G., Y. D. Cui, Z. J. Zhao, J. Li, and B. C. Khoo. 2016. Investigation of airfoil leading edge separation control with nanosecond plasma actuator. *Phys. Rev. Fluids* 1(7): 073501.
- [4] Takashima, K., Y. Zuzeeq, W. R. Lempert, and I. V. Adamovich. 2011. Characterization of a surface dielectric barrier discharge plasma sustained by repetitive nanosecond pulses. *Plasma Sources Sci. Technol.* 20:055009.